Chapter 2

Physics of Tunneling Spectroscopy

Electron tunneling spectroscopy in artificial solid-state tunneling structures was pioneered by the work of Esaki on semiconductor p-n junctions in 1958 [108]. Shortly after, Fisher and Giaever succeeded in fabricating thin-film metal-insulator-metal junctions with reproducible behavior in 1959 [109]. Furthermore, by cooling to below the transition temperature of lead, Giaever [110] directly observed the superconducting energy gap in the differential tunneling conductance (dI/dV vs. V) of an aluminum-oxide-lead junction. The importance of this discovery is two-fold. For one thing, this is the first unequivocal evidence that tunneling current in a well-formed junction accounts entirely for the total current across the junction. For another, it demonstrates that tunneling spectroscopy is a powerful high-energy-resolution tool to study the electronic structures of superconducting material. In this thesis, we employed a specific configuration of tunneling technique, the scanning tunneling spectroscopy, with a normal-metal tip as the counter-electrode to study high-temperature superconductors. To set the foundation for understanding the physics encoded in the tunneling spectra, we first review the theories related to the normal-metal-insulator-superconductor (N-I-S) tunneling process and summarize the equations relevant to data analysis and numerical simulations in later chapters.

2.1 Tunneling Hamiltonian

The most commonly adopted approach to solving the tunneling problem in a many-body system is the transfer Hamiltonian formalism [111, 112, 113] The central assumption of the theory is that the

tunneling barrier separates the two electrodes into two nearly independent subsystems, H_L and H_R, with a weak residual perturbation, H_T, coupling the ground state to the excited states in which a bare electron is transferred from one electrode to the other. The Hamiltonians for the uncoupled left and right electrodes are

$$H_L = \sum_{\mathbf{p}} \epsilon_{\mathbf{p}} c_{\mathbf{p}}^{\dagger} c_{\mathbf{p}} = \mu_L \hat{N}_L + \sum_{p} \xi_{\mathbf{p}} c_{\mathbf{p}}^{\dagger} c_{\mathbf{p}} \tag{2.1}$$

and

$$H_R = \sum_{\mathbf{q}} \epsilon_q c_{\mathbf{q}}^{\dagger} c_{\mathbf{q}} = \mu_R \hat{N}_R + \sum_{q} \xi_{\mathbf{q}} c_{\mathbf{q}}^{\dagger} c_{\mathbf{q}} \tag{2.2}$$

where $c_{\mathbf{p}}$ and $c_{\mathbf{q}}^{\dagger}$ are the particle operators, $\{c_{\mathbf{p}}, c_{\mathbf{q}}^{\dagger}\} = 0$, and

$$H_T = \sum_{\mathbf{p},\mathbf{q}} T_{\mathbf{p},\mathbf{q}} \{c_{\mathbf{p}}^{\dagger} c_{\mathbf{q}} + c_{\mathbf{q}}^{\dagger} c_{\mathbf{p}}\} \tag{2.3}$$

is the tunneling Hamiltonian, also called the transfer Hamiltonian. In Eqs. (2.1)−(2.3), $\epsilon_{\mathbf{p}}$ and $\epsilon_{\mathbf{q}}$ are the single-particle eigen-energies, μ_L and μ_R the chemical potentials, $\hat{N}_L$ and $\hat{N}_R$ the number operators and $\xi_{\mathbf{p}}$ and $\xi_{\mathbf{q}}$ the single-particle eigen-energies referenced to μ_L and μ_R respectively. The tunneling matrix element, $T_{\mathbf{p},\mathbf{q}}$, is the probability amplitude to transfer an electron across the insulating barrier. Using first-order time-dependent perturbation theory, Bardeen [111] showed that $T_{\mathbf{p},\mathbf{q}}$ is determined by the quantum mechanical current density operator evaluated within the barrier,

$$T_{\mathbf{p},\mathbf{q}} = -\frac{\hbar^2}{2m} \int \left\{ \psi_{\mathbf{p}}^* \nabla^2 \psi_{\mathbf{q}} - \psi_{\mathbf{q}}^* \nabla^2 \psi_{\mathbf{p}} \right\} d\tau = -\frac{\hbar^2}{2m} \int \left\{ \psi_{\mathbf{p}}^* \nabla \psi_{\mathbf{q}} - \psi_{\mathbf{q}}^* \nabla \psi_{\mathbf{p}} \right\} \cdot d\vec{S}, \tag{2.4}$$

where $d\tau$ is the volume element, and $d\vec{S}$ is the area element.

After summing over all relevant states, the total tunneling current at the bias voltage V given by the Fermi golden rule is

$$I(V) = \frac{4\pi e}{\hbar} \sum_{\mathbf{p},\mathbf{q}} |T_{\mathbf{p},\mathbf{q}}|^2 \left[f\left(\xi_{\mathbf{p}}\right) - f\left(\xi_{\mathbf{q}}\right) \right] \delta(\xi_{\mathbf{p}} - \xi_{\mathbf{q}} + eV), \tag{2.5}$$

where $\psi_{\mathbf{p}}$ and $\psi_{\mathbf{q}}$ are the single-particle wavefunctions of the left and right electrodes, and f is the Fermi function, $f(\xi) = \frac{1}{1+e^{-\xi/k_BT}}$.

Equation (2.5) is valid only in a non-interacting, single-particle approximation. When generalized to an interacting system that contains all the many-body effects, the tunneling current should be written in terms of the spectral functions of the two electrodes $A_L(p,\omega_{\mathbf{p}})$ and $A_R(q,\omega_{\mathbf{q}})$ [114, 113],

$$I(V) = \frac{4\pi e}{\hbar}\sum_{\mathbf{p},\mathbf{q}}|T_{\mathbf{p},\mathbf{q}}|^2\int\frac{d\omega_{\mathbf{p}}}{2\pi}\int\frac{d\omega_{\mathbf{q}}}{2\pi}\left[f(\omega_{\mathbf{p}})-f(\omega_{\mathbf{q}})\right]A_L(p,\omega_{\mathbf{p}})\,A_R(q,\omega_{\mathbf{q}})\,\delta(\omega_{\mathbf{p}}-\omega_{\mathbf{q}}+eV) \quad (2.6)$$

where $\omega_{\mathbf{p}}$ and $\omega_{\mathbf{q}}$ are two dummy energy variables to be integrated over. In the non-interacting limit, $A_L(p,\omega_{\mathbf{p}}) = 2\pi\delta(\omega_{\mathbf{p}}-\xi_{\mathbf{p}})$, $A_R(q,\omega_{\mathbf{q}}) = 2\pi\delta(\omega_{\mathbf{q}}-\xi_{\mathbf{q}})$, and (2.6) reduces to (2.5).

It is generally assumed that the junction surface is sufficiently smooth so that barrier transmission is specular and that the band structure varies sufficiently slowly so that the WKB approximation is valid [115, 116]. In this case, the evaluation of the matrix element, $T_{\mathbf{p},\mathbf{q}}$, reduces to a one-dimensional tunneling problem. For metallic electrodes with parabolic band structures,

$$\begin{aligned}
&|T_{\mathbf{p},\mathbf{q}}|^2 \approx \tfrac{\partial\xi_{\mathbf{p}}}{\partial\mathbf{p}_L}\tfrac{\partial\xi_{\mathbf{q}}}{\partial\mathbf{q}_L}\,|D(\xi_{\mathbf{p}},\mathbf{p}_T)|^2\,\delta(\mathbf{p}_T-\mathbf{q}_T)\\
&D(\xi_{\mathbf{p}},\mathbf{p}_T) = \exp\left[-\textstyle\int dx\;\kappa(x,\xi_{\mathbf{p}},\mathbf{p}_T)\right] \qquad ,\\
&\kappa(x,\xi_{\mathbf{p}},\mathbf{p}_T) = \sqrt{2m\left[U(x,V)-\xi_{\mathbf{p}}+\hbar^2\mathbf{p}_T^2/2m\right]}
\end{aligned} \quad (2.7)$$

where the subscript L indicates the longitudinal component of the momentum, T indicates the transverse component, D is the transmission coefficient, and κ is the wave vector inside the tunneling barrier $U(x,V)$. Under the assumption that the longitudinal energy $(\xi_{\mathbf{p}}-\hbar^2\mathbf{p}_T^2/2m)$ of the tunneling particle is sufficiently smaller than the barrier height $U(x,V)$, the barrier transmission $D(\xi_{\mathbf{p}},\mathbf{p}_T)$ is approximately a constant.

With Eq. (2.7), when converting the summation over momenta in (2.5) into energy integrals, the

longitudinal band structure is eliminated by the group velocity factors $\frac{\partial \xi_{\mathbf{p}_L}}{\partial p_L}$ and $\frac{\partial \xi_{\mathbf{q}_L}}{\partial q_L}$. As a result,

$$I(V) = \frac{4\pi e}{\hbar} \sum_{\mathbf{p}_T} \int d\xi_{\mathbf{p}} \left| D_{\xi_{\mathbf{p}}, \mathbf{p}_T} \right|^2 \left[f(\xi_{\mathbf{p}}) - f(\xi_{\mathbf{p}} + eV) \right] \propto |D|^2 \int d\xi \left[f(\xi) - f(\xi + eV) \right], \tag{2.8}$$

where the normal state band structure drops out entirely from the expression,[1] and the tunneling current is ohmic at low-bias voltages, $I(V) \propto |D|^2 eV$. For electrodes with more complicate band structures, the cancellation between the Jacobian and the group velocity factors in the tunneling matrix element $T_{\mathbf{p},\mathbf{q}}$ are not complete. Therefore, the tunneling conductance generally contains *convoluted* information of the band structure.[2]

In contrast to the subtleties involved in the interpretation of metal-insulator-metal (N-I-N) tunneling and metal-insulator-semiconductor tunneling spectra in terms of band structure anomalies [115, 117], the N-I-S tunneling current has a surprisingly simple form [110],

$$I(V) \propto \int_{-\infty}^{\infty} d\xi \, |D|^2 \left[f(\xi) - f(\xi + eV) \right] N_S(\xi + eV), \tag{2.9}$$

where $N_S(\xi) \propto \frac{|\xi|}{\sqrt{\xi^2 - \Delta^2}}$ is the density of states of the superconducting electrode, and Δ is the energy gap of the superconductor. Assuming D varies slightly with energy, the differential conductance measures directly the BCS (Bardeen-Cooper-Schrieffer) density of states in the low-temperature limit,

$$\begin{array}{rcl} \frac{dI}{dV}(V) & \propto & |D|^2 \int_{-\infty}^{\infty} d\xi \; N_S(\xi) \left[-\frac{\partial f(eV+\xi)}{\partial (eV)} \right] \\ & \propto & |D|^2 N_S \left(eV \right). \end{array} \tag{2.10}$$

This simple relation between the tunneling conductance and the BCS density of states arises

[1] More precisely, the summation over the transverse momentum $\mathbf{p}_T$ in Eq. (2.8) still contains transverse band structure information. However, for tunneling process between simple metals where a large number of transverse momentum states are available, the exponential function in $D(\xi_{\mathbf{p}}, \mathbf{p}_T)$ limits the effective tunneling to electrons at nearly normal incidence. Consequently, the transverse band structure effect is also suppressed [116].

[2] Most textbooks on many-body physics or superconductivity treat the the tunneling matrix element $T_{\mathbf{p},\mathbf{q}}$ as a constant and pull it out of the momentum summation in Eqs. (2.5) and (2.6). As a result, converting the momentum sum into energy integrals lumps the band structure effect into two density of states factors N_L and N_R in the tunneling current expression

$$I(V) \propto |T|^2 \int d\xi \; N_L(\xi) N_R(\xi + eV) \left[f(\xi) - f(\xi + eV) \right],$$

which strictly speaking is *incorrect*. Using tunneling spectroscopy to determine single-particle band structure information, such as the band edge of semiconductors, generally suffers from the complicated functional form of the tunneling matrix element and other model-dependent uncertainties. More details are given in the classic books on tunneling by Wolf [117] and Duke [115].

from the fact that, although tunneling current does not probe the bare band structure directly, it contains direct information about the spectral function of the many-body system. More explicitly, by identifying $A_L(p,\omega_{\mathbf{p}})$ and $A_R(q,\omega_{\mathbf{q}})$ in (2.6) with the free electron and the superconducting spectral functions, respectively,

$$\begin{aligned} A_L(p,\omega_{\mathbf{p}}) &= 2\pi\delta(\omega_{\mathbf{p}}-\xi_{\mathbf{p}}) \\ A_R(q,\omega_{\mathbf{q}}) &= 2\pi u_{\mathbf{q}}^2\delta(\omega_{\mathbf{q}}-E_{\mathbf{q}})+2\pi v_{\mathbf{q}}^2\delta(\omega_{\mathbf{q}}+E_{\mathbf{q}}), \end{aligned} \tag{2.11}$$

where $u_{\mathbf{q}}$ and $v_{\mathbf{q}}$ are the coherence factors and $E_{\mathbf{q}}=\sqrt{\xi_{\mathbf{q}}^2+\Delta^2}$ the quasiparticle eigen-energy, Eq. (2.6) can be shown to be equivalent to (2.9) under some general assumptions. Interestingly, in the final result, the coherence factors u and v drop out, and a naive semiconductor representation works in the N-I-S tunneling problem.

We postpone the derivation of Eqs. (2.6) and (2.9) to §2.1.1 and end this section by pointing out the limitations of the tunneling Hamiltonian formalism. There are three primary difficulties with the theory [118, 119]. First, there are ambiguities in decomposing the Hamiltonian into H_L, H_R, and H_T. Second, it is impossible to find a set of single-particle wavefunctions that are complete on the left (right) electrode and, at the same time, orthogonal to all the wavefunctions on the right (left) electrode, so that H_L and H_R commute. Third, the first-order time-dependent perturbation theory does not provide an estimate of the errors. Feuchtwang studied these issues thoroughly to investigate the validity of tunneling Hamiltonian formalism [119]. In the report [119], a procedure to calculate Bardeen's transfer matrix element was established and the matrix element was interpreted as a pseudopotential representing the boundary conditions at the interface. The resulting expression for computing the tunneling current formally agrees with the results obtained from the tunneling Hamiltonian approach. Thus, despite the aforementioned problems, the simple tunneling Hamiltonian picture gives us an answer both easy to understand and consistent with the result of a more sophisticated theory. More details are given in [119] and references therein.

2.1.1 Normal-insulator-superconductor tunneling

Giaever's N-I-S tunneling result [110] that states that the differential conductance is directly proportional to the BCS density of states is somewhat surprising because, when calculating most transition rates in a BCS superconductor, the BCS coherence factors generally have important consequences. It is therefore remarkable that they drop out completely from the expression for the tunneling process. This interesting fact stems from normal electrons tunneling into both electron- and hole-branches of the quasiparticles in the superconductors. We now derive (2.6) and (2.9) via the tunneling Hamiltonian approach [112].

The total Hamiltonian is $H = H_N + H_S + H_T$ (N: normal metal, S: superconductor), where $H_T = \sum_{\mathbf{p},\mathbf{q},\sigma}\{T_{\mathbf{p},\mathbf{q}}c^{\dagger}_{\mathbf{p},\sigma}c_{\mathbf{q},\sigma} + T^{*}_{\mathbf{p},\mathbf{q}}c^{\dagger}_{\mathbf{q},\sigma}c_{\mathbf{p},\sigma}\}$. Current flowing through the junction equals to

$$I = \langle \hat{I} \rangle = e\langle \dot{\hat{N}}_S \rangle = \frac{e}{i\hbar}\left\langle \left[\hat{N}_S, H\right]\right\rangle = \frac{e}{i\hbar}\left\langle \left[\hat{N}_S, H_T\right]\right\rangle = \frac{e}{i\hbar}\sum_{\mathbf{p},\mathbf{q},\sigma}\left\langle T_{\mathbf{p},\mathbf{q}}c^{\dagger}_{\mathbf{p},\sigma}c_{\mathbf{q},\sigma} - T^{*}_{\mathbf{p},\mathbf{q}}c^{\dagger}_{\mathbf{q},\sigma}c_{\mathbf{p},\sigma}\right\rangle . \tag{2.12}$$

To first-order in H_T, linear response theory gives

$$I = \frac{e}{\hbar^2}\sum_{\mathbf{p},\mathbf{q},\sigma}\int_{-\infty}^{\infty} dt'\Theta\left(t-t'\right)\left\langle \left[H_T\left(t'\right), T_{\mathbf{p},\mathbf{q}}c^{\dagger}_{\mathbf{p},\sigma}\left(t\right)c_{\mathbf{q},\sigma}\left(t\right) - T^{*}_{\mathbf{p},\mathbf{q}}c^{\dagger}_{\mathbf{q},\sigma}\left(t\right)c_{\mathbf{p},\sigma}\left(t\right)\right]\right\rangle , \tag{2.13}$$

in which $c^{\dagger}_{q,\sigma}\left(t\right)$, $c_{\mathbf{q},\sigma}\left(t\right)$, $c^{\dagger}_{\mathbf{p},\sigma}\left(t\right)$, and $c_{\mathbf{p},\sigma}\left(t\right)$ are defined in the interaction picture. The first two operators are the creation and annihilation operators for electrons in the superconducting electrodes, while the last two are those for the electrons in the normal metal.

In the tunneling process where a definite number of electrons are transferred into a superconductor, Josephson's definition [120] of the quasiparticle operators ($\gamma_{e(h),\sigma}$ and $\gamma^{\dagger}_{e(h),\sigma}$) proved to be superior to the ordinary Bogoliubov operators, for the former create an exact charge e or $-e$ in the

superconductor. The Josephson quasiparticle operators are defined by

$$\begin{aligned}
\gamma^{\dagger}_{e,\mathbf{q}\uparrow} &= u_{\mathbf{q}} c^{\dagger}_{\mathbf{q}\uparrow} - v_q S^{\dagger} c_{-\mathbf{q}\downarrow} \\
\gamma^{\dagger}_{h,\mathbf{q}\uparrow} &= u_{\mathbf{q}} S c^{\dagger}_{\mathbf{q}\uparrow} - v_q c_{-\mathbf{q}\downarrow} = S\gamma^{\dagger}_{e,\mathbf{q}\uparrow} \\
\gamma^{\dagger}_{e,\mathbf{q}\downarrow} &= u_{\mathbf{q}} c^{\dagger}_{-\mathbf{q}\downarrow} + v_q S^{\dagger} c_{\mathbf{q}\uparrow} \\
\gamma^{\dagger}_{h,\mathbf{q}\downarrow} &= u_{\mathbf{q}} S c^{\dagger}_{-\mathbf{q}\downarrow} + v_q c_{\mathbf{q}\uparrow} = S\gamma^{\dagger}_{e,\mathbf{q}\downarrow},
\end{aligned} \tag{2.14}$$

where $S^{\dagger}$ and S are the pair creation and annihilation operators. The inverse operators of (2.14) are

$$\begin{aligned}
c^{\dagger}_{\mathbf{q}\uparrow} &= u_{\mathbf{q}} \gamma^{\dagger}_{e,\mathbf{q}\uparrow} + v_{\mathbf{q}} \gamma_{h,\mathbf{q}\downarrow} \\
c^{\dagger}_{-\mathbf{q}\downarrow} &= u_{\mathbf{q}} \gamma^{\dagger}_{e,\mathbf{q}\downarrow} - v_{\mathbf{q}} \gamma_{h,\mathbf{q}\uparrow}.
\end{aligned} \tag{2.15}$$

Taking into account the chemical potential difference with a bias voltage, $\mu_N - \mu_S = eV$, the unperturbed Hamiltonian and the operators in the interaction picture are written out as

$$\begin{aligned}
H_N &= \mu_N \hat{N}_N + \textstyle\sum_{p\sigma} \xi_{\mathbf{p}} c^{\dagger}_{\mathbf{p}\sigma} c_{\mathbf{p}\sigma} \\
H_S &= \mu_S \hat{N}_S + \textstyle\sum_{q\sigma} E_{\mathbf{q}} \left(\gamma^{\dagger}_{e,\mathbf{q}\sigma} \gamma_{e,\mathbf{q}\sigma} + \gamma^{\dagger}_{h,\mathbf{q}\sigma} \gamma_{h,\mathbf{q}\sigma} \right)
\end{aligned} \tag{2.16}$$

$$\begin{aligned}
c^{\dagger}_{\mathbf{p}\sigma}(t) &= e^{\frac{i}{\hbar} H_N t} c^{\dagger}_{\mathbf{p}\sigma} e^{-\frac{i}{\hbar} H_N t} = e^{\frac{i}{\hbar}(\xi_{\mathbf{p}} + \mu_N) t} c^{\dagger}_{\mathbf{p}\sigma} \\
c_{\mathbf{p}\sigma}(t) &= e^{\frac{i}{\hbar} H_N t} c_{\mathbf{p}\sigma} e^{-\frac{i}{\hbar} H_N t} = e^{-\frac{i}{\hbar}(\xi_{\mathbf{p}} + \mu_N) t} c_{\mathbf{p}\sigma}
\end{aligned} \tag{2.17}$$

$$\begin{aligned}
c^{\dagger}_{\mathbf{q}\uparrow}(t) &= u_{\mathbf{q}} \gamma^{\dagger}_{e,\mathbf{q}\uparrow}(t) + v_{\mathbf{q}} \gamma_{h,\mathbf{q}\downarrow}(t) = u_{\mathbf{q}} e^{\frac{i}{\hbar}(E_{\mathbf{q}} + \mu_S) t} \gamma^{\dagger}_{e,\mathbf{q}\uparrow} + v_{\mathbf{q}} e^{-\frac{i}{\hbar}(E_{\mathbf{q}} - \mu_S) t} \gamma_{h,\mathbf{q}\downarrow} \\
c_{\mathbf{q}\uparrow}(t) &= u_{\mathbf{q}} \gamma_{e,\mathbf{q}\uparrow}(t) + v_{\mathbf{q}} \gamma^{\dagger}_{h,\mathbf{q}\downarrow}(t) = u_{\mathbf{q}} e^{-\frac{i}{\hbar}(E_{\mathbf{q}} + \mu_S) t} \gamma_{e,\mathbf{q}\uparrow} + v_{\mathbf{q}} e^{\frac{i}{\hbar}(E_{\mathbf{q}} - \mu_S) t} \gamma^{\dagger}_{h,\mathbf{q}\downarrow} \\
c^{\dagger}_{\mathbf{q}\downarrow}(t) &= u_{\mathbf{q}} \gamma^{\dagger}_{e,\mathbf{q}\downarrow}(t) - v_{\mathbf{q}} \gamma_{h,\mathbf{q}\uparrow}(t) = u_{\mathbf{q}} e^{\frac{i}{\hbar}(E_{\mathbf{q}} + \mu_S) t} \gamma^{\dagger}_{e,\mathbf{q}\downarrow} - v_{\mathbf{q}} e^{-\frac{i}{\hbar}(E_{\mathbf{q}} - \mu_S) t} \gamma_{h,\mathbf{q}\uparrow} \\
c_{\mathbf{q}\downarrow}(t) &= u_{\mathbf{q}} \gamma_{e,\mathbf{q}\downarrow}(t) - v_{\mathbf{q}} \gamma^{\dagger}_{h,\mathbf{q}\uparrow}(t) = u_{\mathbf{q}} e^{-\frac{i}{\hbar}(E_{\mathbf{q}} + \mu_S) t} \gamma_{e,\mathbf{q}\downarrow} - v_{\mathbf{q}} e^{\frac{i}{\hbar}(E_{\mathbf{q}} - \mu_S) t} \gamma^{\dagger}_{h,\mathbf{q}\uparrow}.
\end{aligned} \tag{2.18}$$

In Eqs (2.16)−Eqs (2.18), $E_{\mathbf{q}} = \sqrt{\xi^2_{\mathbf{q}} + \Delta^2_q}$ is the quasiparticle excitation energy, μ_N and μ_S are the chemical potentials of the normal metal and the superconductor, $\xi_{\mathbf{p}}$ and $\xi_{\mathbf{q}}$ are the single-particle energies referenced to μ_N and μ_S, respectively, and $\hat{N}_N$ and $\hat{N}_S$ are the number operators of the

normal and superconducting electrodes.

Substituting (2.17) and (2.18) into (2.13) and keeping in mind that $\langle c^{\dagger}_{\mathbf{p}\sigma} c_{\mathbf{p}\sigma}\rangle = f(\xi_{\mathbf{p}})$, $\langle c_{\mathbf{p}\sigma} c^{\dagger}_{\mathbf{p}\sigma}\rangle = 1 - f(\xi_{\mathbf{p}})$, $\langle \gamma^{\dagger}_{e,\mathbf{q}\sigma}\gamma_{e,\mathbf{q}\sigma}\rangle = \langle \gamma^{\dagger}_{h,\mathbf{q}\sigma}\gamma_{h,\mathbf{q}\sigma}\rangle = f(E_{\mathbf{q}})$, and $\langle \gamma_{e,\mathbf{q}\sigma}\gamma^{\dagger}_{e,\mathbf{q}\sigma}\rangle = \langle \gamma_{h,\mathbf{q}\sigma}\gamma^{\dagger}_{h,\mathbf{q}\sigma}\rangle = 1 - f(E_{\mathbf{q}})$, we find that the integral in (2.13), $\int_{-\infty}^{\infty} dt'\theta(t-t')\left\langle \left[H_T(t'), T_{\mathbf{p},\mathbf{q}} c^{\dagger}_{\mathbf{p},\sigma}(t)\, c_{\mathbf{q},\sigma}(t) - T^{*}_{\mathbf{p},\mathbf{q}} c^{\dagger}_{\mathbf{q},\sigma}(t)\, c_{\mathbf{p},\sigma}(t)\right]\right\rangle$, equals to

$$\begin{array}{lcl}
i\hbar\frac{u_q^2 f(\xi_{\mathbf{p}})[1-f(E_{\mathbf{q}})]}{\xi_{\mathbf{p}}-E_{\mathbf{q}}+eV+i\delta} & + & i\hbar\frac{v_q^2 f(\xi_{\mathbf{p}}) f(E_{\mathbf{q}})}{\xi_{\mathbf{p}}+E_{\mathbf{q}}+eV+i\delta} \\
-i\hbar\frac{u_q^2 f(\xi_{\mathbf{p}})[1-f(E_{\mathbf{q}})]}{\xi_{\mathbf{p}}-E_{\mathbf{q}}+eV-i\delta} & - & i\hbar\frac{v_q^2 f(\xi_{\mathbf{p}}) f(E_{\mathbf{q}})}{\xi_{\mathbf{p}}+E_{\mathbf{q}}+eV-i\delta} \\
-i\hbar\frac{u_q^2 f(E_{\mathbf{q}})[1-f(\xi_{\mathbf{p}})]}{\xi_{\mathbf{p}}-E_{\mathbf{q}}+eV+i\delta} & - & i\hbar\frac{v_q^2 [1-f(\xi_{\mathbf{p}})][1-f(E_{\mathbf{q}})]}{\xi_{\mathbf{p}}+E_{\mathbf{q}}+eV+i\delta} \\
+i\hbar\frac{u_q^2 f(E_{\mathbf{q}})[1-f(\xi_{\mathbf{p}})]}{\xi_{\mathbf{p}}-E_{\mathbf{q}}+eV-i\delta} & + & i\hbar\frac{v_q^2 [1-f(\xi_{\mathbf{p}})][1-f(E_{\mathbf{q}})]}{\xi_{\mathbf{p}}+E_{\mathbf{q}}+eV-i\delta},
\end{array} \tag{2.19}$$

Recall $\frac{1}{x-x_0\pm i\delta} = P\frac{1}{x-x_0} \mp i\pi\delta(x-x_0)$. The principal integrals in (2.19) cancel each other. Only the delta functions are left. Thus,

$$\begin{array}{rcl}
I & = & \frac{4\pi e}{\hbar}\sum_{\mathbf{p},\mathbf{q}} |T_{\mathbf{p},\mathbf{q}}|^2 \{u_q^2 [f(\xi_{\mathbf{p}}) - f(E_{\mathbf{q}})]\,\delta(\xi_{\mathbf{p}} - E_{\mathbf{q}} + eV) \\
 & & -v_q^2 [1 - f(\xi_{\mathbf{p}}) - f(E_{\mathbf{q}})]\,\delta(\xi_{\mathbf{p}} + E_{\mathbf{q}} + eV)\}.
\end{array} \tag{2.20}$$

For a state $\mathbf{q}^{+}$ with $E_{\mathbf{q}^{+}}$ and $u_{\mathbf{q}^{+}}$, there is another state $\mathbf{q}^{-}$ with the same energy $E_{\mathbf{q}^{-}} = E_{\mathbf{q}^{+}}$ but $\xi_{\mathbf{q}^{-}} = -\xi_{\mathbf{q}^{+}}$, such that $\left|u_{\mathbf{q}^{+}}\right|^2 + \left|u_{\mathbf{q}^{-}}\right|^2 = \left|u_{\mathbf{q}^{+}}\right|^2 + \left|v_{\mathbf{q}^{+}}\right|^2 = 1$, and $\left|v_{\mathbf{q}^{+}}\right|^2 + \left|v_{\mathbf{q}^{-}}\right|^2 = \left|v_{\mathbf{q}^{+}}\right|^2 + \left|u_{\mathbf{q}^{+}}\right|^2 = 1$. Moreover, because $\mathbf{q}^{+}$ and $\mathbf{q}^{-}$ are both near the same point on the Fermi surface, $\left|T_{\mathbf{p},\mathbf{q}^{+}}\right| \approx \left|T_{\mathbf{p},\mathbf{q}^{-}}\right|$. Thus, when summing over all possible $\mathbf{q}$ values, the coherence factors u_q^2 and v_q^2 drop out, and

$$I = \frac{4\pi e}{\hbar}\sum_{\mathbf{p},\mathbf{q}} |T_{\mathbf{p},\mathbf{q}}|^2 [f(\xi_{\mathbf{p}}) - f(E_{\mathbf{q}})]\,\delta(\xi_{\mathbf{p}} - E_{\mathbf{q}} + eV) - [1 - f(\xi_{\mathbf{p}}) - f(E_{\mathbf{q}})]\,\delta(\xi_{\mathbf{p}} + E_{\mathbf{q}} + eV)\}. \tag{2.21}$$

Recall that in Eq. (2.7), assuming specular transmission and bare parabolic band structures, the tunneling matrix element is approximately

$$|T_{\mathbf{p},\mathbf{q}}|^2 \approx \frac{\partial \xi_{\mathbf{p}}}{\partial \mathbf{p}_L}\frac{\partial \xi_{\mathbf{q}}}{\partial \mathbf{q}_L}\,|D(\xi_{\mathbf{p}}, \mathbf{p}_T)|^2\,\delta(\mathbf{p}_T - \mathbf{q}_T), \tag{2.22}$$

where the subscript L indicates the longitudinal component and T the transverse component of the momenta. When converting the momentum summation in (2.21) into energy integrals, assuming $|D|^2$ varies slowly, the tunneling current can be expressed as

$$\begin{aligned} I(V) \quad \propto \quad & |D|^2 N_S(0) \int_{-\infty}^{\infty} d\xi_{\mathbf{p}} \int_0^{\infty} dE_{\mathbf{q}} \left(\frac{\partial \xi_{\mathbf{q}}}{\partial E_{\mathbf{q}}}\right) \{[f(\xi_{\mathbf{p}}) - f(E_{\mathbf{q}})]\, \delta(\xi_{\mathbf{p}} - E_{\mathbf{q}} + eV) \\ & - [1 - f(\xi_{\mathbf{p}}) - f(E_{\mathbf{q}})]\, \delta(\xi_{\mathbf{p}} + E_{\mathbf{q}} + eV)\}, \end{aligned} \tag{2.23}$$

where $N_S(0)$ is the density of states of the superconducting electrode around the Fermi level. Define

$$\frac{N_S(E_{\mathbf{q}})}{N_S(0)} = \left|\frac{\partial \xi_{\mathbf{q}}}{\partial E_{\mathbf{q}}}\right| = \begin{cases} \frac{|E_{\mathbf{q}}|}{\sqrt{E_{\mathbf{q}}^2 - \Delta^2}} & (|E_{\mathbf{q}}| > \Delta) \\ 0 & (|E_{\mathbf{q}}| < \Delta), \end{cases} \tag{2.24}$$

where we have assumed an s-wave superconductor so that Δ is independent of $\mathbf{q}$. We note that by using $1 - f(-\xi_{\mathbf{p}} - eV) = f(\xi_{\mathbf{p}} + eV)$, we arrive at the Giaever's simple formula:

$$\begin{aligned} I(V) \quad \propto \quad & |D|^2 \int_{-\infty}^{\infty} d\xi_{\mathbf{p}} \{N_S(\xi_{\mathbf{p}} + eV)\, [f(\xi_{\mathbf{p}}) - f(\xi_{\mathbf{p}} + eV)]\, \Theta(\xi_{\mathbf{p}} + eV) \\ & - N_S(-\xi_{\mathbf{p}} - eV)\, [1 - f(\xi_{\mathbf{p}}) - f(-\xi_{\mathbf{p}} - eV)]\, [1 - \Theta(\xi_{\mathbf{p}} + eV)]\} \\ \propto \quad & |D|^2 \int_{-\infty}^{\infty} d\xi N_S(\xi + eV)\, [f(\xi) - f(\xi + eV)], \end{aligned} \tag{2.25}$$

The subscript $\mathbf{p}$ is dropped in the very last equation. At low temperatures, (2.25) reduces to

$$\frac{dI}{dV}(V) \propto |D|^2 N_S(eV). \tag{2.26}$$

Thus, measuring the differential conductance spectrum is equivalent to measuring the superconducting density of states.

The transfer Hamiltonian formalism, and hence Eq.(2.26), applies only to tunneling processes with a large barrier height. Furthermore, in deriving (2.26) we sum over the momenta values for both electrodes, so the momentum-dependent information of the tunneling spectral weight is lost. As a result, Eqs.(2.25) and (2.26) are valid only for tunneling into a conventional superconductor whose pairing potential is isotropic, or to those processes that sample over all possible momentum

distribution in an unconventional superconductor, such as the c-axis tunneling of a d-wave superconductor where the surface normal direction of the superconducting electrode aligns along its c crystalline axis.

In the following section, we will introduce another formalism, the generalized Blonder-Tinkham-Klapwijk (BTK) theory, that goes beyond the tunneling limit and analyzes tunneling processes with an arbitrary barrier strength within the same framework. More importantly, BTK theory allows us to simulate the tunneling spectra that retain the momentum-dependent information of an unconventional superconductor. For instance, the zero-bias conductance peak that appears in the tunneling spectrum taken on a {110}-oriented d-wave superconductor reveals existence of nodes and the phase change of the d-wave order parameter, while the U-shape spectral gap in the {100} tunneling spectra of a d-wave superconductor reveals the maximum value of the pairing potential. Thus, BTK theory serves as an important tool to extract the pairing symmetry and pairing potential of any unconventional superconducting order parameter.

2.2 Pairing symmetry and tunneling spectra: generalized Blonder-Tinkham-Klapwijk (BTK) model

Another way of treating the N-I-S tunneling process is to view it as a scattering problem. Analogous to solving the Schrodinger equation in the N-I-N scattering problem, here we solve the Bogoliubov–de Gennes (BdG) equation where the superconducting order parameter serves as a position-dependent off-diagonal potential $\Delta(x)$ and the interface as a diagonal delta-function potential with a variable barrier strength $H\delta(x)$. This approach has the advantage of capturing an important process that the tunneling Hamiltonian failed to, *i.e.*, the Andreev reflection in the low-barrier N-S tunneling limit [121]. Andreev realized that, when an electron (or hole) of energy E approaches the N/S interface from the N region, it will be reflected as a hole (or electron) where $|\Delta|$ rises above E, provided that the length scale over which Δ varies is much larger than the Fermi wavelength. Andreev reflection arises naturally from the Bogoliubov–de Gennes (BdG) equation with a spatially

slowly varying order parameter and a vanishing barrier strength [121].

To take into account the Andreev process and to generalize the N-I-S tunneling problem to acount for arbitrary barrier strength, Blonder *et al.* [122] proposed to calculate the tunneling current through the use of the BdG equation. In the BTK formalism, the BdG equation is set up such that the interface between N and S is modeled as a delta function with a variable dimensionless barrier strength $Z = mH/\hbar^2 k_f$. The order parameter $\Delta(x)$ is approximately zero on the N side and a constant on the S side. By matching the boundary conditions, the probability current of normal reflection $B(E)$ and that of Andreev reflection $A(E)$ are derived [Appendix A]. The tunneling current as a function of the bias voltage V is given in terms of $A(E)$ and $B(E)$,

$$I \propto N_N \int_{-\infty}^{\infty} dE \left[f(E - eV) - f(E) \right] \left[1 + A(E) - B(E) \right]. \tag{2.27}$$

While ordinary reflection associated with $B(E)$ reduces the tunneling current, Andreev reflection associated with $A(E)$ enhances it by transmitting a Cooper pair over the interface for one incident electron.

The Andreev process not only plays an important role in the N-I-S tunneling for a conventional BCS s-wave superconductor in the low-barrier limit, but is also fundamental in the formation of a novel zero-energy surface state of an unconventional superconductor [123]. Kashiwaya and Tanaka generalized the BTK formalism [124, 125, 126] to study the important consequence of this bound state—the zero-bias conductance peak (ZBCP) in the tunneling spectra. It is the ZBCP feature that makes tunneling spectroscopy a phase-sensitive measurement for superconductors with unconventional pairing symmetries.

In this section, we will review the generalized BTK formalism, discuss the origin of the zero-energy bound state and the ZBCP, and present the numerical simulations of the quasiparticle tunneling spectra on a d-wave superconductor along different crystalline orientations. We will also discuss the tunneling results of mixed pairing symmetry superconductors and point out the important signatures in the spectra. A summary of the original BTK formalism for tunneling into an s-wave

superconductor is provided in Appendix A as a reference.

2.2.1 Generalized Blonder-Tinkham-Klapwijk formalism—A mean-field description

The Bogoliubov–de Gennes (BdG) equation generalizes the BCS formalism to treat superconductors with spatially varying pairing strength, chemical potential, and Hartree potential. In an inhomogeneous anisotropic even-parity (such as d-wave) superconductor, the Bogoliubov–de Gennes (BdG) equation reads [127]

$$\begin{aligned} Ef(\mathbf{r}_1) &= \hat{h}_0(\mathbf{r}_1)f(\mathbf{r}_1) + \int d\mathbf{r}_2\Delta(\mathbf{r}_1,\mathbf{r}_2)g(\mathbf{r}_2) \\ Eg(\mathbf{r}_1) &= -\hat{h}_0(\mathbf{r}_1)g(\mathbf{r}_1) + \int d\mathbf{r}_2\Delta(\mathbf{r}_1,\mathbf{r}_2)f(\mathbf{r}_2). \end{aligned} \tag{2.28}$$

To be consistent with the notation of [124, 125], the quasiparticles wavefunction is written as two-component column vector,

$$\Psi(\mathbf{r}_1) = \begin{bmatrix} f(\mathbf{r}_1) \\ g(\mathbf{r}_1) \end{bmatrix}. \tag{2.29}$$

In (2.28), $\hat{h}_0(\mathbf{r}_1) = -\hbar^2\nabla^2_{\mathbf{r}_1}/2m - \mu + V(\mathbf{r}_1)$, μ is the chemical potential, $V(\mathbf{r}_1)$ the Hartree potential, and $\Delta(\mathbf{r}_1,\mathbf{r}_2)$ the pairing potential.

Rewrite the pairing potential in terms of the relative coordinates $\mathbf{r} = \mathbf{r}_1 - \mathbf{r}_2$ and $\mathbf{R} = (\mathbf{r}_1 + \mathbf{r}_2)/2$,

$$\Delta(\mathbf{r}_1,\mathbf{r}_2) = \tilde{\Delta}(\mathbf{r},\mathbf{R}),$$

and Fourier transform $\tilde{\Delta}(\mathbf{r},\mathbf{R})$ into

$$\Delta(\mathbf{k},\mathbf{R}) = \int d\mathbf{r} e^{-i\mathbf{k}\cdot\mathbf{r}}\tilde{\Delta}(\mathbf{r},\mathbf{R}) \equiv \Delta(\hat{\gamma},\mathbf{R}), \tag{2.30}$$

where $\hat{\gamma} = \mathbf{k}/|\mathbf{k}| \approx \mathbf{k}/k_f$ denotes the direction of the quasiparticle momentum and k_f is the magnitude of the Fermi momentum. Then $\Delta(\mathbf{k},\mathbf{R})$ describes, in the quasiclassical approximation,

the pairing potential which quasiparticles with momentum $\mathbf{k}$ experience at position $\mathbf{R}$. Introducing two envelope functions $u(\hat{\gamma}, \mathbf{r}_1)$ and $v(\hat{\gamma}, \mathbf{r}_1)$ to factor away the fast atomic-scale oscillations

$$\Psi(\mathbf{r}_1) = \begin{bmatrix} f(\mathbf{r}_1) \\ g(\mathbf{r}_1) \end{bmatrix} = e^{ik_f \hat{\gamma}\cdot\mathbf{r}_1} \begin{bmatrix} u(\hat{\gamma}, \mathbf{r}_1) \\ v(\hat{\gamma}, \mathbf{r}_1) \end{bmatrix} \tag{2.31}$$

and using Eqs. (2.30) and (2.31), the BdG equation (2.28) is recast into

$$\begin{aligned} Eu(\hat{\gamma}, \mathbf{r}_1) &= -i\tfrac{\hbar^2 k_f}{m}\hat{\gamma}\cdot\nabla_{\mathbf{r}} u(\hat{\gamma}, \mathbf{r}_1) + \Delta(\hat{\gamma}, \mathbf{r}_1) v(\hat{\gamma}, \mathbf{r}_1) \\ Ev(\hat{\gamma}, \mathbf{r}_1) &= i\tfrac{\hbar^2 k_f}{m}\hat{\gamma}\cdot\nabla_{\mathbf{r}} v(\hat{\gamma}, \mathbf{r}_1) + \Delta^*(\hat{\gamma}, \mathbf{r}_1) u(\hat{\gamma}, \mathbf{r}_1). \end{aligned} \tag{2.32}$$

In deriving (2.32) only terms of the lowest order in $(k_f \xi_0)^{-1}$ are retained, since the scale for spatial variation of the pairing potential given by the coherence length ξ_0 is much larger than k_f^{-1}.

Following the logic of the original BTK theory [Appendix A], we first identify the allowed elastic tunneling processes across the N-I-S junction and write down the incident, reflected, and transmitted wavefunctions in the normal and the superconducting electrode. By matching the boundary conditions at the interface, the Andreev reflection coefficient $a(E, \theta)$and the normal reflection coefficient $b(E, \theta)$ are extracted to compute the differential tunneling conductance.

For electrons incident from the normal-metal side with energy E and an angle of incidence θ_N, there are four possible trajectories [Fig. 2.1]. They can be Andreev reflected as holes (A) with an angle θ_N, normal reflected as electrons (B) with an angle of reflection $\theta'_N = \theta_N$, transmitted as electron-like quasiparticles (C) with an angle of refraction θ_S, or transmitted as hole-like quasiparticles (D) with an angle $\theta_S = \theta'_S$. In the normal electrode, the unit vector of the momentum of the incident electrons is denoted as $\hat{\gamma}_N$, that of the reflected electrons as $\hat{\gamma}'_N$, and the pairing potential $\Delta(\hat{\gamma}_N, \mathbf{R}) = \Delta(\hat{\gamma}'_N, \mathbf{R}) = 0$. Solving (2.32) gives us the form of the wavefunction on the N side

$$\Psi_N(\mathbf{r}) = e^{ik_{f_N}\hat{\gamma}_N\cdot\mathbf{r}} e^{i\frac{E}{\hbar k_{f_N}/m}\hat{\gamma}_N\cdot\mathbf{r}} \begin{bmatrix} 1 \\ 0 \end{bmatrix}$$

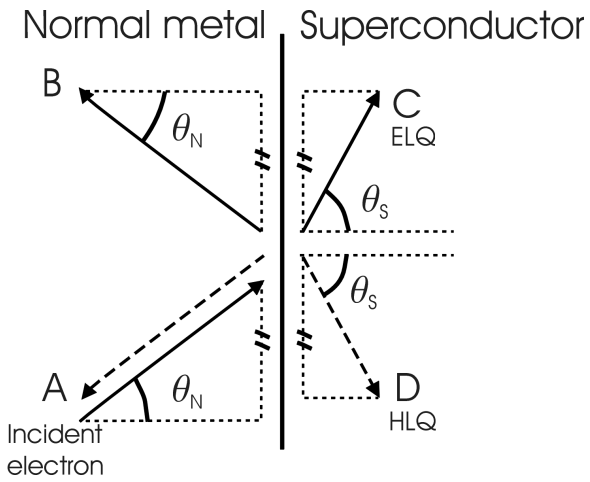

Figure 2.1: Adapted from Fig. 1(b) of [125]. Schematic diagram of the transmission and reflection processes at the N-I-S interface. For an electron incident from the normal metal with an angle of incidence θ_N, it can be Andreev-reflected as a hole (A), normal-reflected as an electron (B) with an angle θ_N, transmitted as an electron-like quasiparticle (ELQ) (C) with an angle θ_S, or transmitted as a hole-like quasiparticle (HLQ) (D). All the electron-like excitations are denoted by solid lines and hole-like excitations dashed lines. The arrows indicate the directions of the group velocities of the particles, and note that, for hole-like quasiparticles, the wave vector and the group velocity point in the opposite directions. The components of the wave vectors parallel to the interface are conserved.

$$+a(E)\, e^{ik_{f_N}\hat{\gamma}_N\cdot\mathbf{r}} e^{-i\frac{E}{\hbar k_{f_N}/m}\hat{\gamma}_N\cdot\mathbf{r}} \begin{bmatrix} 0 \\ 1 \end{bmatrix} + b(E)\, e^{ik_{f_N}\hat{\gamma}'_N\cdot\mathbf{r}} e^{i\frac{E}{\hbar k_{f_N}/m}\hat{\gamma}'_N\cdot\mathbf{r}} \begin{bmatrix} 1 \\ 0 \end{bmatrix}, \tag{2.33}$$

where a is the amplitude for Andreev reflection, b the amplitude for normal reflection, and k_{f_N} the Fermi momentum in the normal electrode. Since $k_{f_N} \gg Em/\hbar k_{f_N}$, (2.33) is approximately

$$\Psi_N(\mathbf{r}) \approx e^{ik_{f_N}\hat{\gamma}_N\cdot\mathbf{r}} \begin{bmatrix} 1 \\ 0 \end{bmatrix} + a(E)\, e^{ik_{f_N}\hat{\gamma}_N\cdot\mathbf{r}} \begin{bmatrix} 0 \\ 1 \end{bmatrix} + b(E)\, e^{ik_{f_N}\hat{\gamma}'_N\cdot\mathbf{r}} \begin{bmatrix} 1 \\ 0 \end{bmatrix}. \tag{2.34}$$

In the superconducting electrode, we denote the unit vector of the momentum of the transmitted electron-like quasiparticles (ELQ) as $\hat{\gamma}_S$, that of the transmitted hole-like quasiparticles (HLQ) as $\hat{\gamma}'_S$, the pairing potential experienced by the "ELQ's" as $\Delta(\hat{\gamma}_S, \mathbf{R}) = |\Delta(\hat{\gamma}_S, \mathbf{R})|\, e^{i\phi(\hat{\gamma}_S)} = |\Delta_+|\, e^{i\phi_+}$, and that experienced by the "HLQ's" as $\Delta(\hat{\gamma}'_S, \mathbf{R}) = |\Delta(\hat{\gamma}'_S, \mathbf{R})|\, e^{i\phi(\hat{\gamma}'_S)} = |\Delta_-|\, e^{i\phi_-}$. Then the

wavefunction for the transmitted electron-like and hole-like quasiparticles reads

$$\Psi_S(\mathbf{r}) = c(E)\, e^{ik_{f_S}\hat{\gamma}_S\cdot\mathbf{r}} e^{i\frac{\sqrt{E^2-|\Delta_+|^2}}{\hbar k_{f_S}/m}\hat{\gamma}_S\cdot\mathbf{r}} \begin{bmatrix} \sqrt{\frac{E+\sqrt{E^2-|\Delta_+|^2}}{2E}} \\ e^{-i\phi_+}\sqrt{\frac{E-\sqrt{E^2-|\Delta_+|^2}}{2E}} \end{bmatrix}$$

$$+d(E)\, e^{ik_{f_S}\hat{\gamma}'_S\cdot\mathbf{r}} e^{-i\frac{\sqrt{E^2-|\Delta_-|^2}}{\hbar k_{f_S}/m}\hat{\gamma}'_S\cdot\mathbf{r}} \begin{bmatrix} e^{i\phi_-}\sqrt{\frac{E-\sqrt{E^2-|\Delta_-|^2}}{2E}} \\ \sqrt{\frac{E+\sqrt{E^2-|\Delta_-|^2}}{2E}} \end{bmatrix} \tag{2.35}$$

$$\Psi_S(\mathbf{r}) \approx c(E)\, e^{ik_{f_S}\hat{\gamma}_S\cdot\mathbf{r}} \begin{bmatrix} \sqrt{\frac{E+\sqrt{E^2-|\Delta_+|^2}}{2E}} \\ e^{-i\phi_+}\sqrt{\frac{E-\sqrt{E^2-|\Delta_+|^2}}{2E}} \end{bmatrix} + d(E)\, e^{ik_{f_S}\hat{\gamma}'_S\cdot\mathbf{r}} \begin{bmatrix} e^{i\phi_-}\sqrt{\frac{E-\sqrt{E^2-|\Delta_-|^2}}{2E}} \\ \sqrt{\frac{E+\sqrt{E^2-|\Delta_-|^2}}{2E}} \end{bmatrix}, \tag{2.36}$$

where k_{f_S} is the Fermi momentum in the superconducting electrode.

The insulating interface is modeled as a δ-function Hartree potential $V(\mathbf{r}) = H\delta(\mathbf{r})$. By solving for the coefficients $a(E) - d(E)$ under the boundary conditions (1) $\Psi^N(0) = \Psi^S(0) = \Psi(0)$ and (2) $\frac{\hbar}{2m}\frac{d\Psi^S(0)}{dx} - \frac{\hbar}{2m}\frac{d\Psi^N(0)}{dx} = H\Psi(0)$, and taking into account the momentum conservation parallel to the interface, we arrive at the following expression for the probability current tunneling across the N-I-S junction at zero temperature:

$$\sigma_S(E,\theta_N) \equiv \sigma_N\left[1 + |a(E,\theta_N)|^2 - |b(E,\theta_N)|^2\right] = \sigma_N \frac{1 + \sigma_N|\Gamma_+|^2 + (\sigma_N - 1)|\Gamma_+\Gamma_-|^2}{\left|1 + (\sigma_N - 1)\Gamma_+\Gamma_- e^{i(\phi_- - \phi_+)}\right|^2}, \tag{2.37}$$

where

$$\begin{aligned} \Gamma_\pm &= \frac{E - \sqrt{E^2 - |\Delta_\pm|^2}}{|\Delta_\pm|}, \\ \sigma_N &= \frac{4\frac{k_{f_S}}{k_{f_N}}\frac{\cos\theta_S}{\cos\theta_N}}{(1+\frac{k_{f_S}}{k_{f_N}}\frac{\cos\theta_S}{\cos\theta_N})^2 + 4(\frac{Z}{\cos\theta_N})^2}, \\ Z &= \frac{mH}{\hbar^2 k_{f_N}}. \end{aligned}$$

In an s-wave superconductor where $\Delta_+ = \Delta_- = \Delta$, Eq.(2.37) reduces to the original BTK formula (A.12), (A.13), and (A.14).

2.2.2 Tunneling spectra of a d-wave superconductor and the Andreev bound state

Having derived (2.37), we can now calculate the tunneling conductance spectra of superconductors with unconventional pairing symmetries in a real scanning tunneling spectroscopy (STS) experiment. Taking into account a finite transverse momentum distribution for the incident particles by considering a finite tunneling cone β, the resulting tunneling conductance is

$$\frac{dI}{dV}(V) \propto \int d\theta \left[1 + |a(E,\theta)|^2 - |b(E,\theta)|^2\right] e^{-\frac{\theta^2}{\beta^2}}. \tag{2.38}$$

For simplicity, $k_{f_S}/k_{f_N} \approx 1$ is assumed, and thus $\theta_N \approx \theta_S \equiv \theta$. Since in the STS configuration we usually operate in the tunneling limit, the following simulations are done with a large effective barrier height. We focus on the spectra of d-, $(d+s)$-, $(d+is)$-, and $(d+id')$-wave superconductors which are the most relevant to later chapters on the hole-doped cuprates.

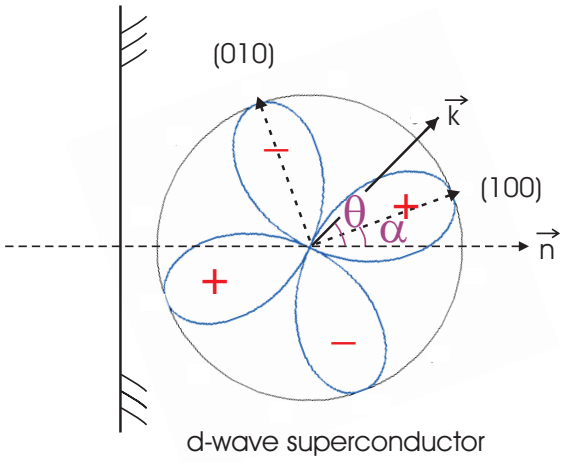

Figure 2.2: Momentum dependence of a d-wave pairing potential. $\Delta(\mathbf{k}) = \Delta(\theta) = \Delta_d \cos(2\theta - 2\alpha)$. θ is the angle between the surface normal and the wave vector $\mathbf{k}$, and α is the angle between the surface normal and (100)-axis of the superconductor.

In a d-wave superconductor, $\Delta(\mathbf{k}) = \Delta(\theta) = \Delta_d \cos(2\theta)$ [Fig. 2.2]. The pairing potentials Δ_+

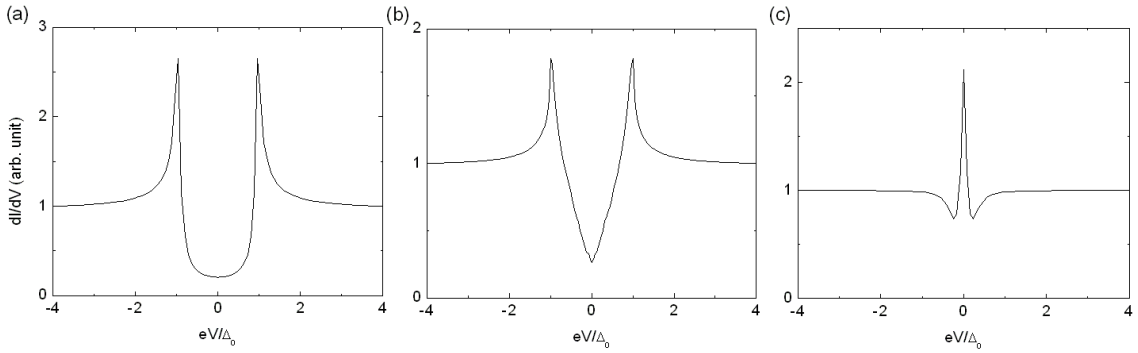

Figure 2.3: Simulated tunneling spectra of a d-wave superconductor taken with the average quasiparticle momentum parallel to (a) the anti-nodal (100) direction, (b) the c-axis (001) direction, and (c) the nodal (110) direction. The scanning tunneling spectroscopy configuration is usually operated in the tunneling limit. Thus, these BTK simulation curves are carried out with a large effective barrier height.

and Δ_- that the ELQ's and the HLQ's experience are

$$\begin{aligned} \Delta_+ &= \Delta_d \cos(2\theta - 2\alpha) \\ \Delta_- &= \Delta_d \cos(2\theta + 2\alpha), \end{aligned} \tag{2.39}$$

where α is the angle between the normal vector of the interface and (100)-axis of the superconductor. When the normal vector $\vec{n}$ of the interface is oriented along the anti-nodal (100) or (010) direction (*i.e.*, $\alpha = 0$ and $\Delta_+ = \Delta_-$), the tunneling spectrum shows a U-shape feature as in a BCS superconductor, with two coherence peaks located at the maximal pairing potential $\pm\Delta_d$ and no density of states found within the gap [Fig. 2.3(a)]. When $\vec{n}$ is parallel to the (001)-axis, the incident electrons sample over all possible θ values and hence the tunneling cone completely opens up in this case ($\beta \approx \infty$). In addition, the conservation of the momentum parallel to the interface implies that $\Delta_+ = \Delta_-$ for c-axis tunneling. The resulting spectrum has a V-shape feature with the coherence peaks located at $\pm\Delta_d$ [Fig. 2.3(b)].

Most interestingly, when the normal vector $\vec{n}$ of the junction surface is oriented along the nodal (110) direction, the pairing potentials experienced by the ELQ's and the HLQ's are opposite in sign, $\Delta_+ = -\Delta_-$. Consequently, the tunneling spectrum displays a conductance peak at zero bias [Fig. 2.3(c)]. In the high-barrier low-transmission limit ($\sigma_N \to 0$), the normalized tunneling conductance reduces to the surface density of states [125, 126]. Therefore, the zero-bias conductance

peak (ZBCP) reflects the existence of a zero-energy surface state, called the Andreev bound state (ABS), at the superconductor-insulator interface.

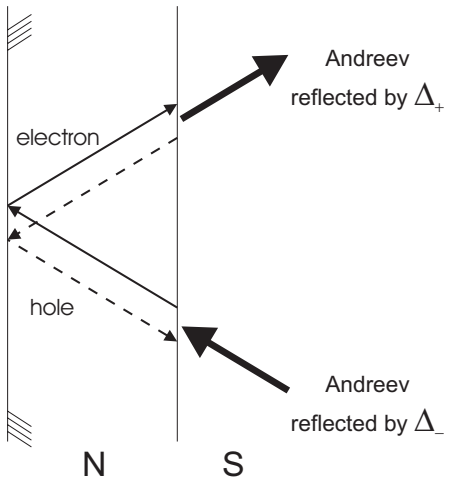

Figure 2.4: Trajectories of the Andreev bound states at the surface of a d-wave superconductor. (Taken from Fig. 7 of [126].) The existence of the surface states is stable even in the limit of vanishing normal metallic layer. The solid lines denote the trajectories of the electrons, and the dashed lines the trajectories of the holes. When the electrons Andreev reflected from the N/S interface, they experience a pairing potential Δ_+, while the Andreev reflection of holes experiences Δ_-. When the normal vector of the interface is parallel to the nodal (110) direction, the two pairing potentials have equal magnitude but opposite signs, giving rise to a bound state at $E = 0$.

Mathematically, the energy of the bound state is determined by the zero of the denominator in (2.37),

$$1 - \Gamma_+\Gamma_- e^{i(\phi_- - \phi_+)} = 0, \sigma_N \to 0. \tag{2.40}$$

Given that $\phi_- - \phi_+ = \pi$ and $|\Delta_+| = |\Delta_-|$, the bound state energy is always at $E = 0$. Physically, an intuitive visualization of the formation of ABS at the surface of a d-wave superconductor is given by [126]. As illustrated in Fig. 2.4, assume that the surface of the superconductor is capped with a thin layer of normal metal of thickness d_N. The trajectories of the quasiparticles form closed loops through two Andreev reflections at the N/S interface (one converting electrons to holes and the other converting holes to electrons) and two specular reflections at the surface. Applying the quantization condition that the phase shift is a multiple of 2π for a bound quasiparticle along a closed path of the classical trajectory, and taking into account that the phase shifts picked up by the two Andreev reflections are different because of different pairing potentials the ELQ's and the HLQ's experience,

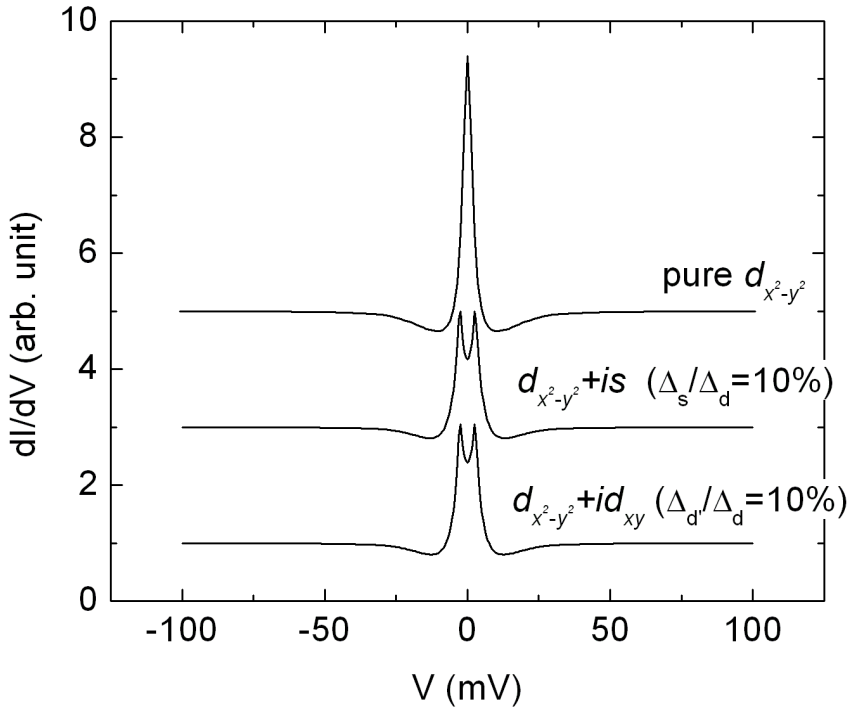

Figure 2.5: Tunneling spectra taken along the nodal direction for different pairing symmetries. The spectra of pure d-wave and $(d+is)$-wave superconductors have been shifted for clarity. As shown in the figure, a small imaginary component (*e.g.*, 10% the gap value of a 30 meV d-wave superconductor) can produce appreciable splitting ($>$ 6 meV) of the zero-bias conductance peak (ZBCP). For a $(d+id')$ superconductor, the amount of the ZBCP splitting is comparable to that of a $(d+is)$ superconductor, provided that the percentage of symmetry mixing is the same. For a $(d+s)$-wave superconductor (not shown), the shape and width of the ZBCP is indistinguishable from that of a pure d-wave superconductor within experimental resolution.

we obtain the equation that dictates the bound state energy:

$$-\tan^{-1}\left(\frac{\sqrt{|\Delta_+|^2-E^2}}{E}\right)-\tan^{-1}\left(\frac{\sqrt{|\Delta_-|^2-E^2}}{E}\right)-(\phi_+-\phi_-)+2\phi_N=2n\pi, \tag{2.41}$$

where n is an integer and ϕ_N is the phase shift accumulated when traveling around the metallic layer, $\phi_N = md_N E/(\hbar^2 k_{f_N})$. In a real system where the thickness of the metallic layer is vanishingly small, the quantization condition (2.41) reduces to (2.40), and N-I-S tunneling along (110) into these zero-energy surface states gives rise to the ZBCP in the conductance spectrum.

In the presence of a small imaginary component mixed to the predominantly d-wave order parameter, *e.g.*, $d+is$, the degeneracy of the zero-energy bound states is lifted because of broken time-reversal symmetry. The resulting splitting in the ZBCP provides an estimate of the weight of

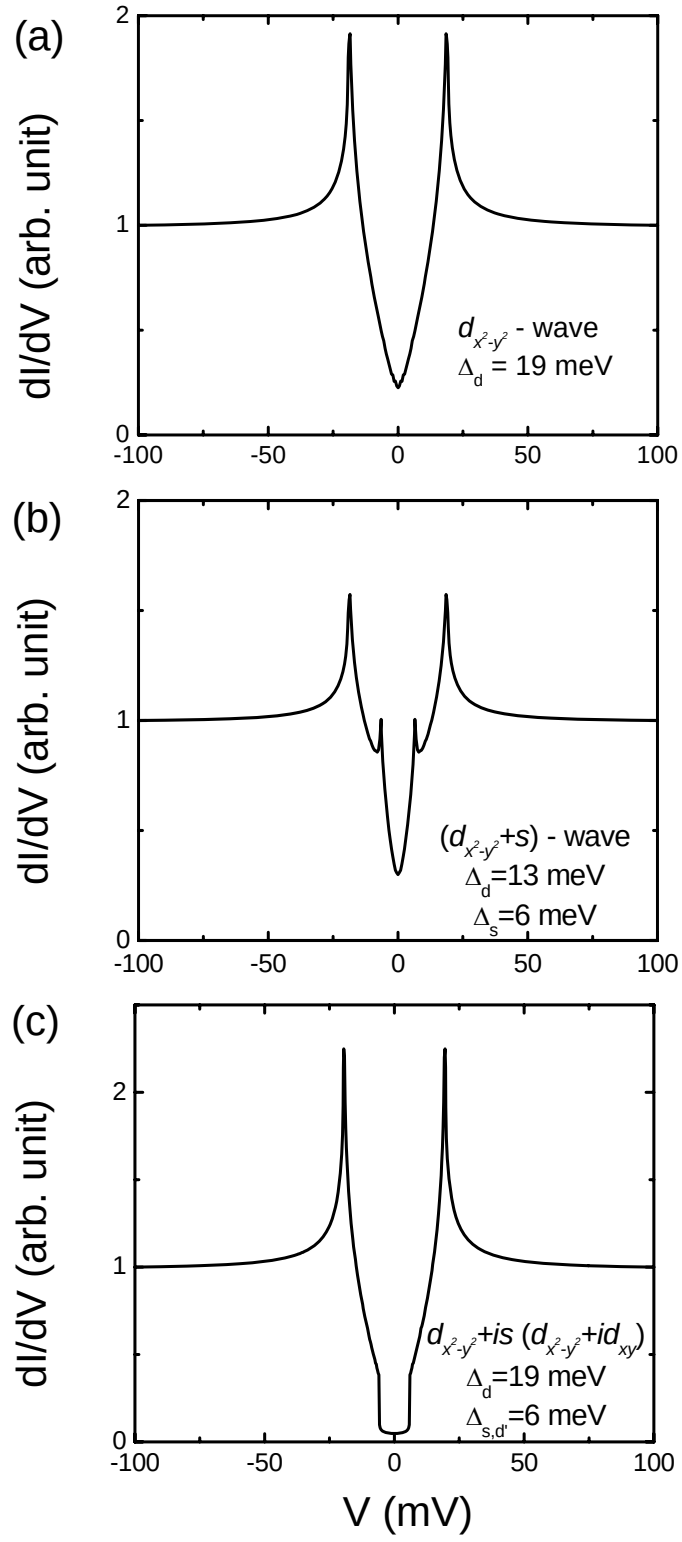

Figure 2.6: Tunneling spectra taken along the c-axis. (a) Tunneling spectrum of a pure d-wave, (b) a $(d+s)$-wave, and (c) a $(d+is)$ or $(d+id')$ superconductor. The gap values are chosen so that the position of the coherence peaks and the subgap features stays the same for all three figures.

the imaginary component [Fig. 2.5(a)]. On the contrary, as shown in [Fig. 2.5(b)], because time-reversal symmetry is still respected, a small real s-component mixing does not break the degeneracy. Therefore, tunneling spectra taken along the nodal direction cannot distinguish between d-wave and $d+s$-wave pairing symmetry.

Although the existence of a small s-wave component does not modify the shape and the magnitude of the ZBCP, it does have other observational consequences on the tunneling spectra. For example, tunneling spectra along (100) and (010) reveal two different gap values, $\Delta_d \pm \Delta_s$. Similarly, the c-axis tunneling spectrum of a $(d+s)$-wave superconductor shows two corresponding sets of coherence peaks [Fig. 2.6(b)] in contrast to that of the pure d-wave superconductor [Fig. 2.6(a)]. For comparison, the c-axis tunneling spectrum of a $(d+is)$-wave superconductor is plotted in Fig. 2.6(c). Owing to the small imaginary component mixing, the low-energy excitation is fully gapped within the secondary pairing potential Δ_s (or $\Delta_{d'}$). Therefore, around zero bias the c-axis tunneling shows a small U-shape feature [Fig. 2.6(c)] in contrast to the V-shape feature in the d- and $(d+s)$-wave cases.

As a final remark, we note that the generalized BTK theory is based on the mean-field Bogoliubov–de Gennes equation. Therefore, quantum/thermal fluctuations and residual interactions, such as quasiparticle scattering and quasiparticle coupling with the bosonic modes of the system, are not accounted for.

In conclusion, the existence of a zero-energy Andreev surface state turns quasiparticle tunneling spectroscopy into a phase-sensitive technique to uncover the sign change of the order parameter across the nodal axis in an unconventional superconductor. At the mean-field level, the symmetry of the order parameter, the magnitude of the pairing potential and the amount of secondary symmetry mixing can be extracted by means of the generalized Blonder-Tinkham-Klapwijk formalism. We will present an example of applying the BTK formalism to study the tunneling spectra of the hole-doped cuprate $YBa_2Cu_3O_{6+\delta}$ [§4], which demonstrates that, for YBCO, mean-field theory is a good approximation and the Bogoliubov quasiparticle description captures most of the important physics in the superconducting state. In contrast, deviation from the BTK formalism is observed in the

electron-doped $Sr_{1-x}La_xCuO_2$, indicating that the mean-field approximation is not adequate for this compound. The implication of the breakdown will be discussed in detail in §5 and §6.